The Astrophysical Journal, 659:812–828, 2007 April 10

VECTOR MAGNETIC FIELDS OF MOVING MAGNETIC FEATURES AND FLUX REMOVAL FROM A SUNSPOT

M. Kubo,[1,2,3] T. Shimizu,[1] and S. Tsuneta[3]
Received 2005 October 27; accepted 2006 December 31

ABSTRACT

Moving magnetic features (MMFs) are small photospheric magnetic elements moving outward in the zone (moat region) surrounding mature sunspots. Vector magnetic fields and horizontal motion of the classical MMFs (called isolated MMFs hereafter) are investigated using coordinated ASP and MDI observations. Their magnetic and velocity properties are compared to nearby magnetic features, including moat fields surrounding the isolated MMFs and penumbral uncombed structure. The moat fields are defined as nonisolated MMFs because they also move outward from sunspots. The nonisolated MMFs have nearly horizontal magnetic fields of both polarities. We find that the isolated MMFs located on the lines extrapolated from the horizontal component of the uncombed structure have magnetic fields similar to the nonisolated MMFs. This suggests that the MMFs with nearly horizontal fields are intersections of horizontal fields extended from the penumbra with the photospheric surface. We find clear evidence that the isolated MMFs located on the lines extrapolated from the vertical component of the uncombed structure have vertical field lines with polarity same as the sunspot. This correspondence shows that such MMFs are detached from the spine (vertical) component of the penumbra. We estimate that the magnetic flux carried by the vertical MMFs is about 1–3 times larger than the flux loss of the sunspot. We suggest that the isolated vertical MMFs alone can transport sufficient magnetic flux and are responsible for the disappearance and disintegration of the sunspot.

Subject headings: Sun: magnetic fields — Sun: photosphere — sunspots

Online material: color figures

1. INTRODUCTION

Mature sunspots are surrounded by a moat region with outward flows. The outer radius of the moat region is typically about twice the sunspot radius (Brickhouse & Labonte 1988). Numerous magnetic features called moving magnetic features (MMFs) are observed in the moat region. MMFs move radially from around the outer boundary of the sunspot penumbra. In this study, we examine which moving features are responsible for removal of magnetic flux from sunspots.

MMFs appear everywhere in the moat region with unipolar or bipolar magnetic configurations. MMFs tend to appear as a pair of opposite polarities near the outer edge of penumbra (Harvey & Harvey 1973; Ryutova et al. 1998; Zhang et al. 2003), and at least some MMFs are born inside the penumbra (Sainz Dalda & Martínez Pillet 2005). MMFs often appear in association with the Evershed flows at dark penumbral filaments, which are more horizontal to the surface than bright penumbral filaments (Lee 1992; Ryutova et al. 1998). Cabrera Solana et al. (2006) showed that Evershed clouds moved radially outward in the penumbra and became MMFs once they reached the outer sunspot boundary. Bonet et al. (2004) reported that many G-band bright points located near the penumbra were born close to or at the end of dark penumbral filaments. MMFs arrive at the outer boundary of the moat region, or they vanish in the moat region (Harvey & Harvey 1973; Zhang et al. 2003). The measured horizontal velocity of MMFs ranges from 0.1 to 1.5 km s^{-1} (Harvey & Harvey 1973; Nye et al. 1984; Brickhouse & Labonte 1988; Lee 1992; Zhang et al. 1992, 2003; Ryutova et al. 1998).

Three magnetic configurations have been proposed so far to explain bipolar MMFs: Ω-loop (Harvey & Harvey 1973; Nye et al. 1984; Ryutova et al. 1998; Shine & Title 2001; Thomas et al. 2002b; Weiss et al. 2004), U-loop (Zhang et al. 2003), and O-loop (Wilson 1986). The bipolar pair corresponds to the erupted part of an horizontally oriented flux tube below the photosphere in the Ω-loop configuration, whereas it corresponds to the downward kink of the magnetic canopy of sunspots in the U-loop configuration. The moat flow moves isolated magnetic rings from the penumbral edge in the O-loop configuration.

Unipolar MMFs are less studied than bipolar MMFs. Shine & Title (2001) show that there are two types of unipolar MMFs in addition to bipolar MMFs (which they call type I MMFs). Unipolar MMFs with polarity same as the central sunspot (type II MMFs) are shed from the edge of the sunspot and move outward through the moat region, while unipolar MMFs with polarity opposite to that of the sunspot (type III MMFs) have higher speed than others and disappear within several minutes. Thomas et al. (2002b) and Weiss et al. (2004) propose that type III MMFs correspond to intersections of the submerged penumbral flux and type II MMFs are formed as a result of the detached penumbral spines.

Properties of MMFs such as lifetime, location, and motion have been studied using only longitudinal magnetograms in previous works. Our study uses Stokes profile observations coordinated with series of longitudinal magnetograms (§ 2). In addition to the classical MMFs described in § 1, the magnetic fields of moat region with horizontal motion are investigated in this study. Such moat fields are defined as another type of MMFs (§ 4). Vector magnetic fields and motion of MMFs are described, and are compared with penumbral magnetic fields. We estimate how much magnetic flux is carried away from the sunspot by MMFs in terms of a decay

[1] Institute of Space and Astronautical Science, Japan Aerospace Exploration Agency, Sagamihara, Kanagawa 229-8510, Japan.
[2] Department of Astronomy, Graduate School of Science, University of Tokyo, Tokyo 113-0033, Japan.
[3] National Astronomical Observatory of Japan, Tokyo 181-8588, Japan. This work was completed while affiliated at University of Tokyo/NAOJ.

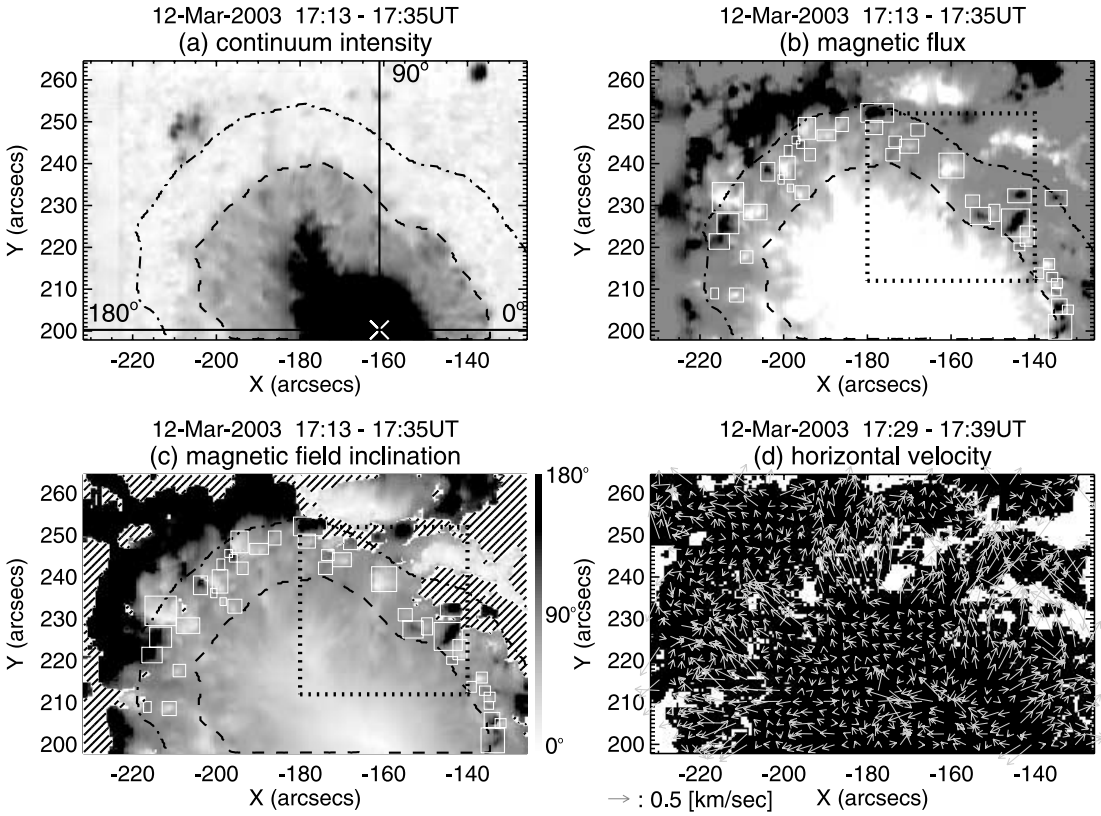

FIG. 1.—Sunspot in active region NOAA 10306 on 2003 March 12. (*a*) Continuum intensity, (*b*) magnetic flux, and (*c*) magnetic field inclination map derived from the ASP data. The magnetic flux map shows the quantity $F = f|\boldsymbol{B}| \cos\gamma$ for each pixel, where f, $|\boldsymbol{B}|$, and γ are the filling factor, the field strength, and the inclination, respectively. White (black) is for positive (negative) polarity in the magnetic flux map. The dashed line represents the outer boundary of the penumbra. The dash-dotted line represents the position of 15″ radial distance from the penumbral outer boundary. The position angle, which is measured counterclockwise around the azimuth center (*cross in panel a*) of the sunspot from the solar west, is used to produce Figs. 4 and 8. The solid boxes show the isolated MMFs. The dotted box indicates the field of view for Fig. 5. The degree of polarization is less than 0.4% for the hatched areas with oblique lines in panel *c*. Panel *d* shows horizontal velocity map derived from the MDI magnetograms in the high-resolution mode with the local cross-correlation technique. White areas represent invalid MDI data areas, which have magnetic flux less than 10 G or maximum correlation coefficients smaller than 0.9. Positions are given with respect to the center of the solar disk. [*See the electronic edition of the Journal for a color version of this figure.*]

rate of the sunspot in § 5. Finally, we discuss their association with penumbral magnetic and velocity structures and importance of MMFs in the decaying process of sunspots in § 6.

2. OBSERVATIONS

We carried out observations of a well-developed sunspot in active region NOAA 10306 with the Advanced Stokes Polarimeter (ASP; Elmore et al. 1992), the Michelson Doppler Imager (MDI; Scherrer et al. 1995) on board the *Solar and Heliospheric Observatory* (*SOHO*; Domingo et al. 1995), and the *Transition Region and Coronal Explorer* (*TRACE*; Handy et al. 1999) during 2003 March 11–17. The ASP data set taken with good seeing conditions in 17 : 13–17 : 35 UT on 2003 March 12 was examined in detail (see Fig. 1). The sunspot was located near the disk center (N6°, E10°) and was rather simple in circular shape. The sunspot gradually divided into two spots after March 13, evolving into more complicated structure.

The ASP is a spectropolarimeter measuring the full polarization state (Stokes I, Q, U, V) of the Zeeman sensitive Fe I λ6301.5 and Fe I λ6302.5 lines with a typical signal/noise ratio (S/N) $\sim$ 1000 (Lites et al. 1993). The instrument is installed as one of the focal plane instruments of the Richard B. Dunn Solar Telescope (DST) of the National Solar Observatory at Sacramento Peak, New Mexico, in the United States. The spectral resolution was 25 mÅ at 6302 Å, and the CCD pixel sampling was 12 mÅ. The slit scanning step size was 0.525″, and integration time per one slit position was about 4 s. The mapping to cover the sunspot required 20 minutes. The spatial resolution was about 1″–3″, depending on the atmospheric seeing, although the pixel size is 0.37″.

MDI provided longitudinal magnetograms in high-resolution mode with 1 minute cadence during the ASP observing period on 12 March. The field of view was 640″ × 320″ with pixel sampling of 0.625″. The MDI magnetograms were used for visually identifying classical MMFs and evaluating horizontal velocity of moving features.

TRACE mainly provided coronal images in Fe IX/x λ171 line with high spatial resolution ($\sim$1″). The Fe IX/x λ171 lines are formed at temperatures of about 1 MK. The field of view was 512″ × 512″ with pixel size of 0″.5. The *TRACE* images were taken at a cadence of about 1 minute. *TRACE* also obtained white light and 1600 Å images with a cadence of about 10 minutes. Coronal activities around the sunspot are reported in the Appendix.

3. ANALYSIS

3.1. *Derivation of Magnetic Field Vector*

After observed Stokes profiles were corrected for instrumental polarization, the magnetic field vector and thermodynamic parameters were derived from the calibrated Stokes profiles. We used a nonlinear least-squares fitting code developed by the High Alitude Observatory (HAO; Skumanich & Lites 1987; Lites & Skumanich 1990) to fit analytical Stokes profiles to the observed profiles. Twelve physical values (azimuth angle, inclination angle, and strength of the magnetic field; wavelength centers of the two Fe I

lines; Doppler width; damping constant; ratio of line center to continuum opacity; slope and surface value of the source function; filling factor [the areal percentage of each pixel occupied by magnetic atmosphere]; and wavelength shift of the nonpolarized profile) were free parameters in the HAO code. In this study, we focus on the inclination (γ), the field strength ($|\boldsymbol{B}|$), and line of sight Doppler velocity ($v_{\rm los}$). More detailed descriptions of the calibration and analysis of the ASP Stokes data can be found in Kubo et al. (2003).

The inclination is defined in the coordinate system of the "local frame," in which one views the region from directly above the solar surface. Inclinations of 0° and 180° represent magnetic fields vertical to the solar surface, with 0° corresponding to the direction away from the surface. When magnetic fields are parallel to the solar surface, inclination is 90°. The 180° ambiguity in the azimuth angle of magnetic field was resolved as follows. At first, the azimuth was selected such that it agreed with potential field as much as possible. The potential field was computed using the line-of-sight component of magnetic field as a boundary condition. Next, we interactively examined and selected the azimuth to reduce point-by-point discontinuities of the azimuth and the inclination by using the AZAM software (Lites et al. 1995). Magnetic fields diverged from pores and sunspots with positive polarity or converged to them for negative polarity. The azimuth was determined such that magnetic fields were continuous and were connected to the plages or sunspots for the rest of the area.

The Doppler velocity was determined from the center position of the Stokes profiles of Fe I λ6302.5 in the magnetized atmosphere. The telluric lines located just besides the Zeeman-sensitive Fe I lines were used to calibrate the absolute wavelength. The zero-velocity in the Doppler velocity was given by averaging the center position of the Fe I λ6302.5 line over the entire field of view. Thus, the Doppler velocity represented the velocity relative to the mean rotational velocity at the position of the observation. We did not correct convective blueshift, because relative velocity around the penumbral outer boundary is important in this paper. Positive Doppler velocities correspond to blueshifts.

3.2. *Horizontal Velocity of Magnetic Features*

Horizontal velocity of magnetic features was obtained by applying a local correlation tracking method (November & Simon 1988) to MDI magnetograms (Chae et al. 2001; Sakamoto 2004). The two images were made by averaging five sequential MDI longitudinal magnetograms (5 minutes) obtained at 17 : 29 and 17 : 39 on 2003 March 12 in order to reduce noise. The 1 σ noise for a single MDI magnetogram was typically 20 G, and it reduced to 8.9 G for the averaged magnetogram (Scherrer et al. 1995; Krivova & Solanki 2004). Horizontal velocities with up to 1.5 km s^{-1} could be detected in this calculation. When a pixel of the MDI magnetogram had magnetic flux less than 10 G, the horizontal velocity for the pixel was not computed. When the cross-correlation coefficient was less than 0.9, the horizontal velocity for the pixel was not computed either. The apodization window was taken to be Gaussian with 4″ FWHM for the computation of the horizontal velocity.

3.3. *Image Co-Alignment*

To investigate the relationship between magnetic field and horizontal velocity of MMFs, or to estimate the magnetic flux carried away from the sunspot due to MMFs, it is necessary to align the ASP and MDI data with high accuracy. Image cross-correlation was used to match the ASP continuum image to the MDI continuum image taken at the time closest to the time of the ASP observation. When the *TRACE* 171 Å image was compared with the ASP and MDI data, the *TRACE* white light image was used for image cross-correlation. The accuracy of co-alignment among the ASP, MDI, and *TRACE* data is estimated to be 1″.

4. MAGNETIC FIELDS AND HORIZONTAL MOTION OF MMFs

4.1. *Identification of MMFs*

The penumbral outer boundary of the sunspot is shown by a dashed line in Figure 1*a*. This boundary corresponds to a continuum intensity level ($I_c = 0.87$) between the quiet area ($I_c = 1.0$) and the penumbra ($I_c = 0.8$). A zone surrounding the penumbra is called the moat region, which is defined to have the width of 15″ in this study (Fig. 1*a*, *dash-dotted line*). The moat region analyzed here corresponds to the limb-side moat region. Small pores or spots are seen outside the moat region. The cross in Figure 1*a* is the apparent center of the sunspot, which is used as the center of azimuth position angle.

There are numerous small magnetic features in the moat region (Fig. 1*b*). By visually inspecting the time sequence of MDI magnetograms, we pick up small magnetic features moving radially outward in the moat region. The selected features are marked by solid boxes in Figure 1 and are called isolated MMFs in this paper. They are isolated from the penumbra and the surroundings. Magnetic features with size less than 1″ in diameter are not chosen as isolated MMFs. We identify 21 isolated MMFs with positive polarity, which is the same as the polarity of the sunspot, and 21 isolated MMFs with negative polarity.

Most of the moat region surrounding the isolated MMFs also have polarization signals higher than the threshold (0.4%). The horizontal velocity map obtained from the MDI magnetograms shows that magnetic features other than the isolated MMFs also move outward (Fig. 1*d*). Such magnetic features are called nonisolated MMFs in this paper. The nonisolated MMFs meet the following conditions: (1) Maximum correlation coefficient when we compute horizontal velocities with the MDI magnetograms is larger than 0.9. (2) the magnetic flux is larger than 10 G in the two MDI magnetograms averaged over 5 minutes. (3) The degree of polarization is larger than 0.4% in the ASP data. (4) The ASP line-of-sight magnetic flux map has polarity same as that of the MDI magnetogram for the same position. Pixels not meeting the fourth condition are only 2% of all the pixels. Such pixels may be caused by the measurement errors of magnetic fields, time difference, or atmospheric seeing. When a pixel does not meet all of the four conditions above, the pixel is called a bad pixel in this paper. The nonisolated MMFs appear to be the same phenomena as the magnetic "swell" discovered by Sainz Dalda & Martínez Pillet (2005). However, our study for the first time has investigated properties of such diffuse and ubiquitous moving moat fields by using observations with vector magnetic fields.

4.2. *Magnetic Fields of MMFs*

We describe magnetic properties of the isolated and nonisolated MMFs from the ASP observations, and they are compared with penumbral magnetic fields.

4.2.1. *Magnetic Fields of Nonisolated MMFs*

Magnetic fields of the nonisolated MMFs are nearly horizontal to the solar surface ($\gamma = 60^\circ - 105^\circ$), and their field strength is weak ($|\boldsymbol{B}| < 1000$ G) (Fig. 2*a*). The peak in the histogram of inclination is shifted about 10° to positive polarity, which is same as the polarity of the sunspot. Sainz Dalda & Martínez Pillet (2005) have interpreted that moving horizontal magnetic fields predominantly pervade the moat region using MDI longitudinal magnetograms.

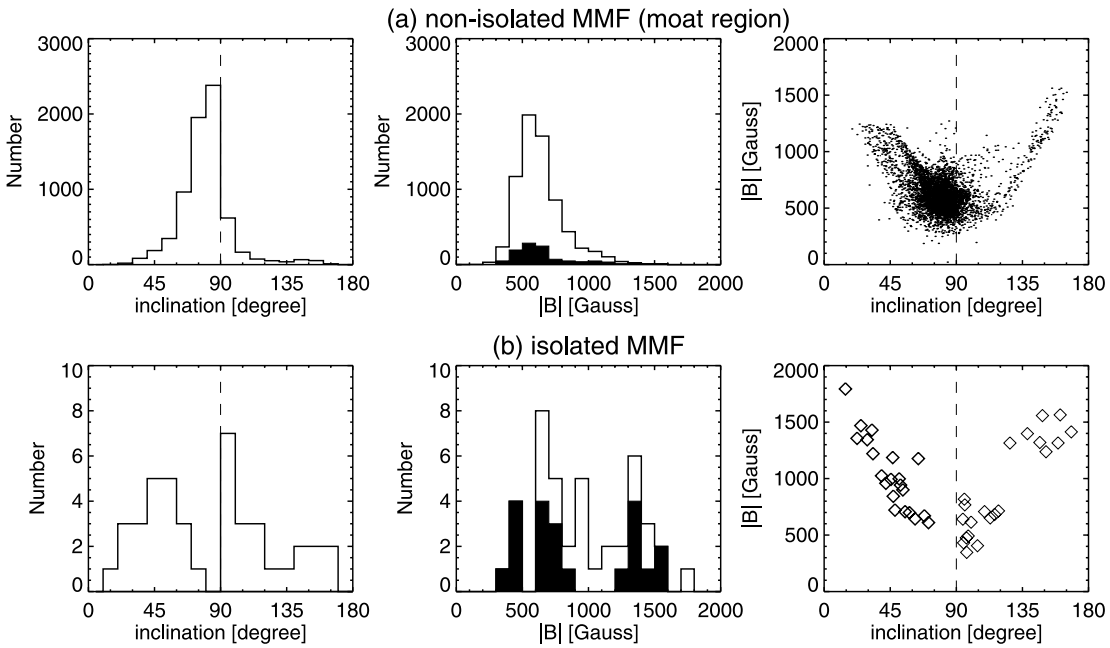

FIG. 2.—Histograms of magnetic field inclination γ (*left*) and field strength $|\boldsymbol{B}|$ (*middle*), and their relationship (*right*) for (*a*) nonisolated MMFs and (*b*) isolated MMFs. Filled distributions show the magnetic field strength for negative polarity. Physical parameters of the isolated MMFs are measured at the center of magnetic flux.

Our observation with vector magnetic field confirms their interpretation. The average inclination of the nonisolated MMFs gradually changes from positive to negative polarity with increasing distance from the penumbral outer boundary (Fig. 3*a*), and their average field strength fluctuates between 600 and 850 G throughout the moat region (Fig. 3*b*).

4.2.2. *Magnetic Fields of Isolated MMFs*

Many of the isolated MMFs with negative polarity have magnetic fields horizontal to the solar surface ($\gamma = 90^\circ$–135°) and weak field strength ($|\boldsymbol{B}| < 1000$ G), as shown in Figure 2*b*. The histogram of the inclination for the isolated MMFs with positive polarity ($0^\circ < \gamma < 90^\circ$) has a peak around 45°. The isolated MMFs with vertical magnetic fields ($0^\circ < \gamma < 45^\circ$ and $135^\circ < \gamma < 180^\circ$) have strong field strength ($|\boldsymbol{B}| > 1000$ G). The percentage of isolated MMFs with vertical magnetic fields is larger than that of nonisolated MMFs with vertical magnetic fields. There are no isolated MMFs with inclinations of 70°–90° probably because magnetic features can be identified as isolated MMFs only when they have polarity opposite to the ambient magnetic fields or when they have magnetic fields with inclinations that differ by more than about 15° from that of the ambient magnetic fields.

4.2.3. *Relation between MMFs and Penumbra*

High spatial-resolution continuum images show that the outer boundary of the sunspot penumbra has narrow radial features. The narrow radial features called spines (Lites et al. 1993) have more vertical magnetic fields than the surroundings, and horizontal magnetic fields and relatively vertical fields are alternately located at the outer boundary of the penumbra (Degenhardt & Wiehr 1991; Title et al. 1993; Lites et al. 1993; Rimmele 1995; Stanchfield et al. 1997; Westendorp Plaza et al. 2001a, 2001b; Mathew et al. 2003). Such penumbral magnetic field structure is called uncombed structure, fluted structure, or interlocking-comb structure. These structures are observed in our sunspot as shown by the dashed lines in Figure 4*a*. The spines are up to 40° more vertical than their

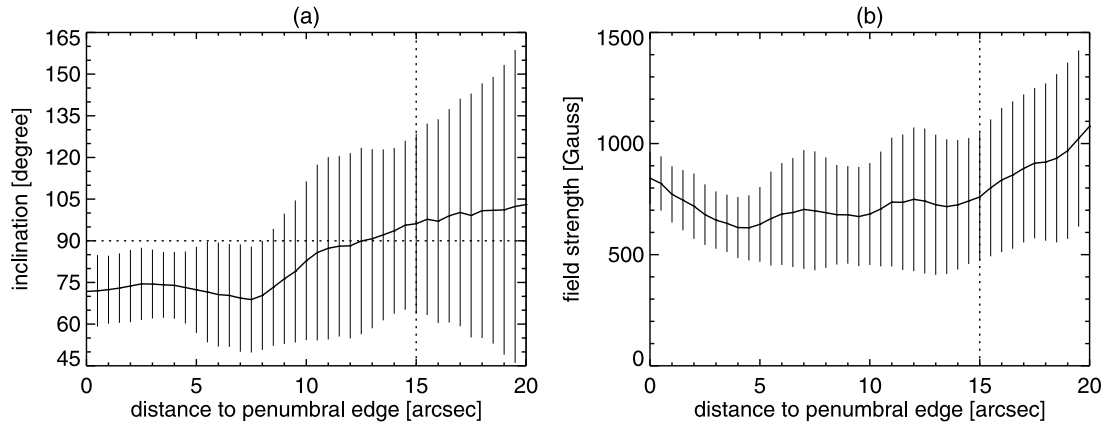

FIG. 3.—(*a*) Averaged variation of magnetic field inclination and (*b*) field strength for the nonisolated MMFs as functions of distance from the penumbral edge. The magnetic field inclination and field strength are averaged for position angle ψ_p of 60°–180° at each distance. The vertical bars on the curves represent the rms fluctuations of the field inclination and field strength at different radial distances. The vertical dotted line represents the outer boundary of the moat region.

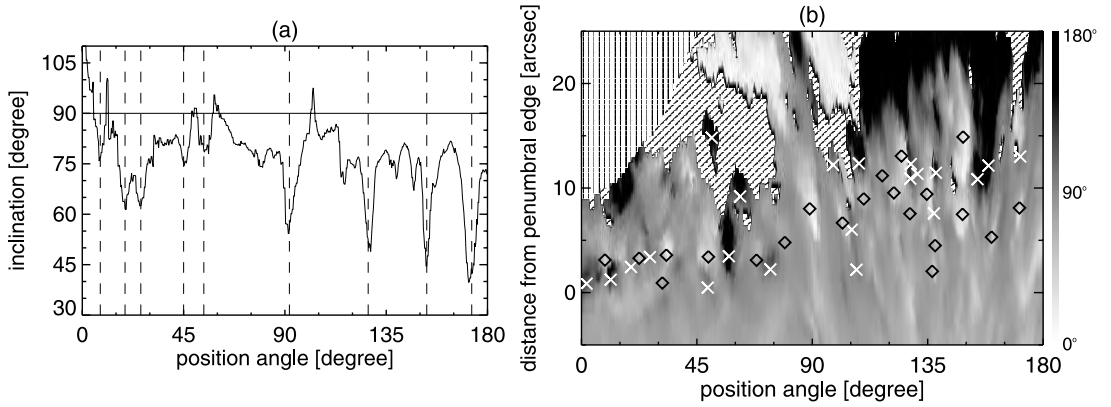

FIG. 4.—(*a*) Variation of magnetic field inclination γ obtained with the ASP along the penumbral outer boundary (Fig. 1*c*, *dashed line*). The vertical dashed lines correspond to spines of the penumbra. (*b*) Magnetic field inclination for the moat region in radial distance (d_p) from the penumbral outer boundary-position angle (ψ_p)-plane. The diamonds and crosses show positions of the isolated MMFs with positive and negative polarities, respectively. The hatched areas with vertical lines and oblique lines represent the area out of the ASP field of view and the area where degree of polarization is less than 0.4%, respectively. [*See the electronic edition of the Journal for a color version of this figure.*]

surroundings at the penumbral outer boundary. Figure 4*b* shows that the spines of the penumbra extend up to around $d_p = 5''$. The spines for the position angle ψ_p of 90°–180° are apparently more vertical than those for the position angle ψ_p of 0°–90°.

We find that the isolated MMFs located on the lines extrapolated from the spines have more vertical magnetic fields than the surroundings, and their magnetic fields are more vertical than those of the spines at around the penumbral outer boundary. This tendency is clearly observed for the position angle ψ_p of 90°–180°, where magnetic fields of the spines are more vertical. These MMFs have only positive polarity, which is the same as the polarity of the sunspot, and there is not any isolated MMF with negative polarity on the lines extrapolated from the spines in the zone less than about $10''$ from the penumbral outer boundary. Time series of the MDI longitudinal magnetograms show that they separate from the spines and move outward in the moat region (Fig. 5). Thus, the isolated MMFs located on the lines extrapolated from the vertical component of the penumbral uncombed structure correspond to the

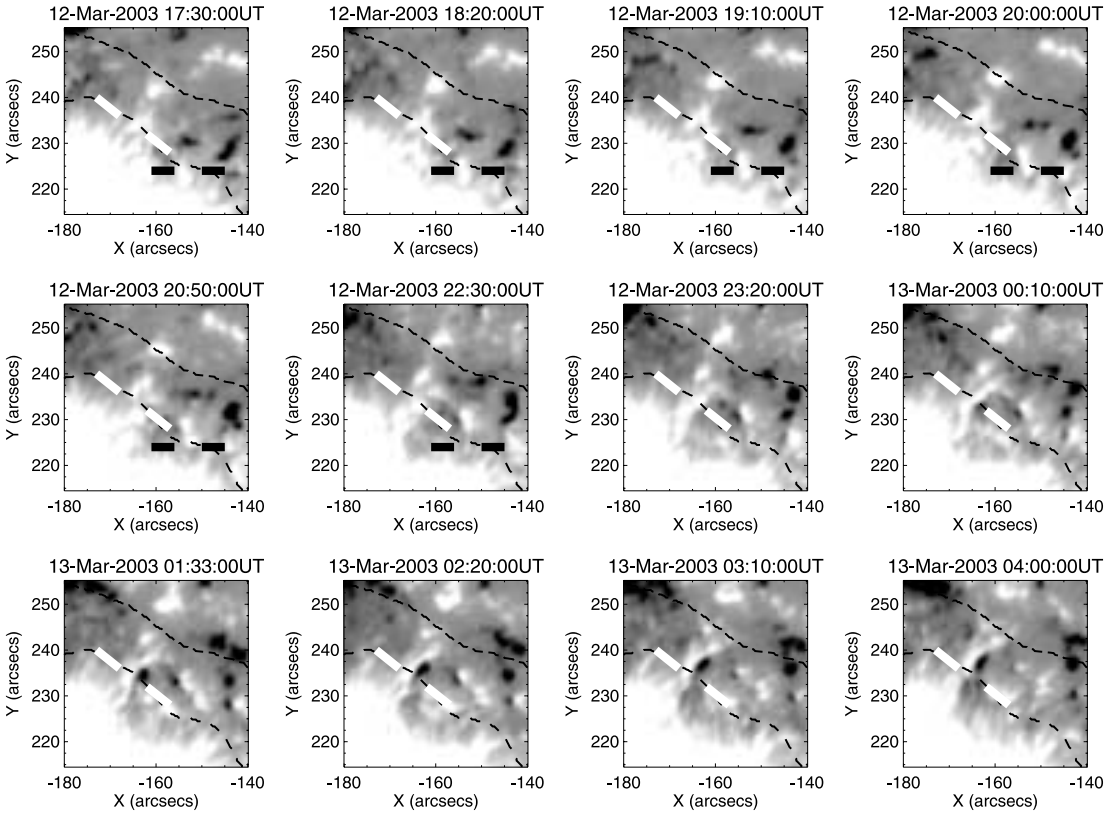

FIG. 5.—Time series of MDI longitudinal magnetograms showing that isolated-MMFs separate from the penumbral spines (*areas between the two solid white recatngles and between the two solid black rectangles*). The field of view is identical to the box in Fig. 1. The dashed and dash-dotted lines represent the outer boundary of the penumbra and the position $15''$ away from the penumbral outer boundary, respectively. Such lines correspond to those in Fig. 1.

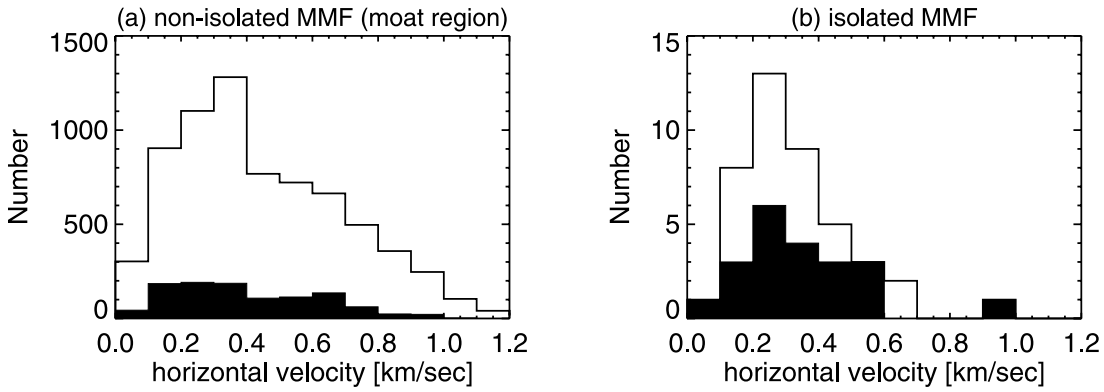

FIG. 6.—(*a*) Histograms of horizontal velocity v_h for the nonisolated MMFs and (*b*) the isolated MMFs. Filled distributions show the horizontal velocities for negative polarity. The horizontal velocities of the isolated MMFs are measured at the center of magnetic flux. The horizontal velocities are averaged over 3×3 pixels (1.1″) at each point to take into account the alignment error (1″) between the ASP and MDI images.

type II MMFs in the classification by Shine & Title (2001). The magnetic field structure of such MMFs is discussed in § 6.1 (see also Fig. 12).

We also find that many of the isolated MMFs located on the lines extrapolated from the horizontal component of the penumbral uncombed structure have nearly horizontal magnetic fields. They have both negative and positive polarities. They are observed from the penumbral edge throughout the outer boundary of the moat region. Some isolated MMFs having vertical magnetic fields with negative polarity are located on the same lines, and they are observed only around the outer boundary of the moat region. One of them around the position angle $\psi_p \sim 50^\circ$ is located near the penumbral outer boundary against the rule. The isolated MMFs with negative polarity may be negative elements of type I (bipolar) MMFs. We cannot identify clear bipolar structures for the isolated MMFs with negative polarity. This is discussed in § 6.2.

4.3. *Horizontal Motion of MMFs*

Horizontal motions of MMFs are obtained with the local correlation technique from the MDI longitudinal magnetograms. We describe horizontal motions of MMFs and their relationship with magnetic field properties of MMFs. We then compare horizontal motions of the MMFs with magnetic and velocity fields of the penumbra.

4.3.1. *Horizontal Velocity of Isolated and Nonisolated MMFs*

Horizontal velocity for the nonisolated MMFs is 0.45 km s^{-1} on average, ranging from 0.1 to 1.0 km s^{-1}, while the average horizontal velocity for the isolated MMFs is 0.34 km s^{-1}. Figure 6 shows that the percentage of isolated MMFs with high horizontal velocity (>0.4 km s^{-1}) is smaller than that of the nonisolated MMFs. The average and range of the horizontal velocity obtained here slightly depend on the FWHM of the apodization window (November & Simon 1988). We set this value to be 4″, so that the horizontal velocity is similar to previous works: Brickhouse & Labonte (1988) studied 200 MMFs in seven sunspots, giving a wide distribution of both moat flows and MMF motions ranging from 0.1 to 1.0 km s^{-1} with an average of about 0.5 km s^{-1}. Recently, Zhang et al. (2003) identified 144 bipolar MMFs in the MDI magnetograms at high-resolution mode, and their horizontal velocities ranged from 0.1 to 0.9 km s^{-1} with an average of 0.45 km s^{-1}.

4.3.2. *Relation between Horizontal Velocity and Magnetic Fields of MMFs*

The magnetic fields of the nonisolated MMFs with high horizontal velocity ($v_h > 0.4$ km s^{-1}) are nearly horizontal ($\gamma = 60^\circ$–110°) and their field strength is weak ($|\boldsymbol{B}| < 1000$ G), as shown in Figure 7. Magnetic fields of the nonisolated MMFs with small horizontal velocity ($v_h < 0.4$ km s^{-1}) have widely distributed inclination and field strength.

Most of the high-speed isolated MMFs ($v_h > 0.4$ km s^{-1}) with negative polarity have magnetic fields with horizontal orientation ($\gamma = 90^\circ$–105°) and weak field strength ($|\boldsymbol{B}| < 700$ G), while the high-speed isolated MMFs with positive polarity have the inclination of about 60° with the field strength of about 1000 G (Fig. 7*b*). The isolated MMFs with vertical magnetic fields ($0^\circ < \gamma < 45^\circ$ and $135^\circ < \gamma < 180^\circ$) have horizontal velocities of less than 0.4 km s^{-1}.

4.3.3. *Relation between MMFs and Penumbra*

The nonisolated MMFs can be found on lines extrapolated from both the spine and the horizontal component of the penumbral uncombed structure (Fig. 4*b*). Horizontal velocities of the nonisolated and isolated MMFs are higher on the lines extrapolated from the horizontal component of the uncombed structure than on lines extrapolated from the spine in general (Fig. 8*b*). The MMFs with high horizontal velocity ($v_h > 0.4$ km s^{-1}) are located in the zone less than about 10″ from the penumbral outer boundary. The MMFs located on the lines extrapolated from the spine or outside the high horizontal velocity channels have slower horizontal velocity ($v_h < 0.4$ km s^{-1}). Shine & Title (2001) show that narrow regions called collar flows have outward velocities (1 km s^{-1}) higher than the rest (0.4–0.6 km s^{-1}) of the moat region. The high horizontal velocity channels correspond to their collar flows. Zhang et al. (1992) have reported that unipolar MMFs with polarity same as the sunspot move slower than bipolar MMFs. This result is consistent with our observations that the isolated MMFs located on the lines extrapolated from the spines have only polarity same as the sunspot and their horizontal velocities are slower than those of the isolated MMFs with polarity opposite to the sunspot in the moat region near the penumbra.

The high-speed MMFs with polarity opposite to the sunspot correspond to the type III MMFs in the classification by Shine & Title (2001). However, the high-speed MMFs also have polarity same as the sunspot in our observations. Many of the high-speed MMFs with polarity same as the sunspot are the nonisolated MMFs. The high-speed MMFs with both polarities have similar magnetic properties. Previous observations indicate that the penumbral magnetic fields return to below the solar surface around the outer edge of the penumbra (Westendorp Plaza et al. 2001a, 2001b; Bellot Rubio et al. 2004; Borrero et al. 2004, 2005). Thomas et al. (2002b) and Weiss et al. (2004) have proposed that the type III MMFs

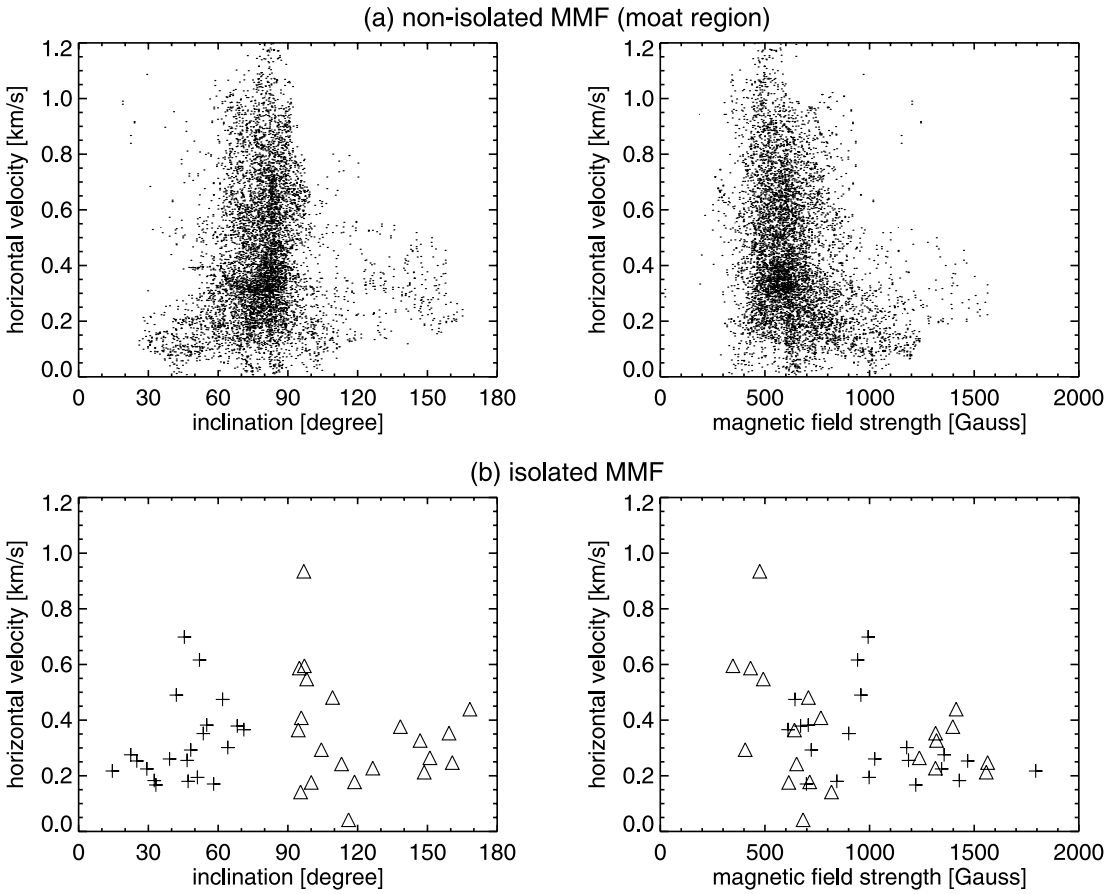

FIG. 7.—Horizontal velocity v_h as a function of magnetic field inclination γ (*left*) and field strength $|\boldsymbol{B}|$ (*right*) for the (*a*) nonisolated MMFs and (*b*) the isolated MMFs. Physical parameters of the isolated MMFs are measured at the center of magnetic flux. The cross and triangle show the isolated MMFs with positive and negative polarities, respectively. The horizontal velocities are averaged over the 3×3 pixels ($1.1''$) at each point.

correspond to the intersections of the returned penumbral flux at the photospheric surface. Our observations show that the high-speed MMFs are not only located at the intersections of the returned penumbral flux (polarity opposite to the sunspot) but also their surroundings (polarity same as the sunspot).

Large Doppler motions called the Evershed flow are observed in the horizontal component of the penumbral uncombed structure by previous authors (Degenhardt & Wiehr 1991; Title et al. 1993; Lites et al. 1993; Rimmele 1995; Stanchfield et al. 1997; Westendorp Plaza et al. 2001a, 2001b; Mathew et al. 2003; Bellot Rubio et al. 2003, 2004). The Evershed flow is an horizontal outflow in the photospheric layers of the penumbra. Figure 8*c* shows that high Doppler velocities (up to 1 km s^{-1}) are observed in between the spines. These are line-of-sight component of the Evershed flows. The average of the Doppler velocity gradually changes from positive (blueshift) to negative (redshift) with increasing position angle. This apparent change is due to the direction of the Evershed flows relative to the line-of-sight direction. We find that high horizontal velocity channels are located on the lines extrapolated from the Evershed channels (Fig. 8*d*). Many authors have proposed that outward motions of MMFs are driven by the Evershed flows (Ryutova et al. 1998; Martínez Pillet 2002; Thomas et al. 2002a; Schlichenmaier 2002; Zhang et al. 2003).

4.4. *Comparison between Isolated and Nonisolated MMFs*

Magnetic fields and motion of the isolated and nonisolated MMFs are summarized in Table 1. We find that these properties of MMFs depend on the location of the MMFs with respect to the uncombed structure of the penumbra. The isolated MMFs with vertical magnetic fields are located on the lines extrapolated from the spines of the penumbra. These MMFs have polarity same as the sunspot, and correspond to the type II MMFs. The isolated MMFs located on the lines extrapolated from the horizontal component of the penumbral uncombed structure have nearly horizontal magnetic fields. These MMFs have both polarities. Their horizontal velocity is higher than the surroundings in the zone between penumbral edge and the middle of the moat region. Such high-speed MMFs are located on the lines extrapolated from the Evershed channels. The high-speed MMFs with polarity opposite to the sunspot correspond to the type III MMFs. Some isolated MMFs having vertical magnetic fields with polarity opposite to the sunspot are located on the lines extrapolated from the horizontal component of the penumbral uncombed structure. They are only located in the outer area of the moat region.

The nonisolated MMFs have nearly horizontal magnetic fields. They tend to have polarity same as the sunspot in the inner and middle of the moat region, while they have polarity opposite to the sunspot in the outer area of the moat region. They have high horizontal velocities on the lines extrapolated from the Evershed channels.

The isolated MMFs with vertical magnetic fields are clearly distinguished from the nonisolated MMFs, while the properties of the isolated MMFs with horizontal magnetic fields are similar to those of the nonisolated MMFs. Thus, the isolated MMFs with horizontal

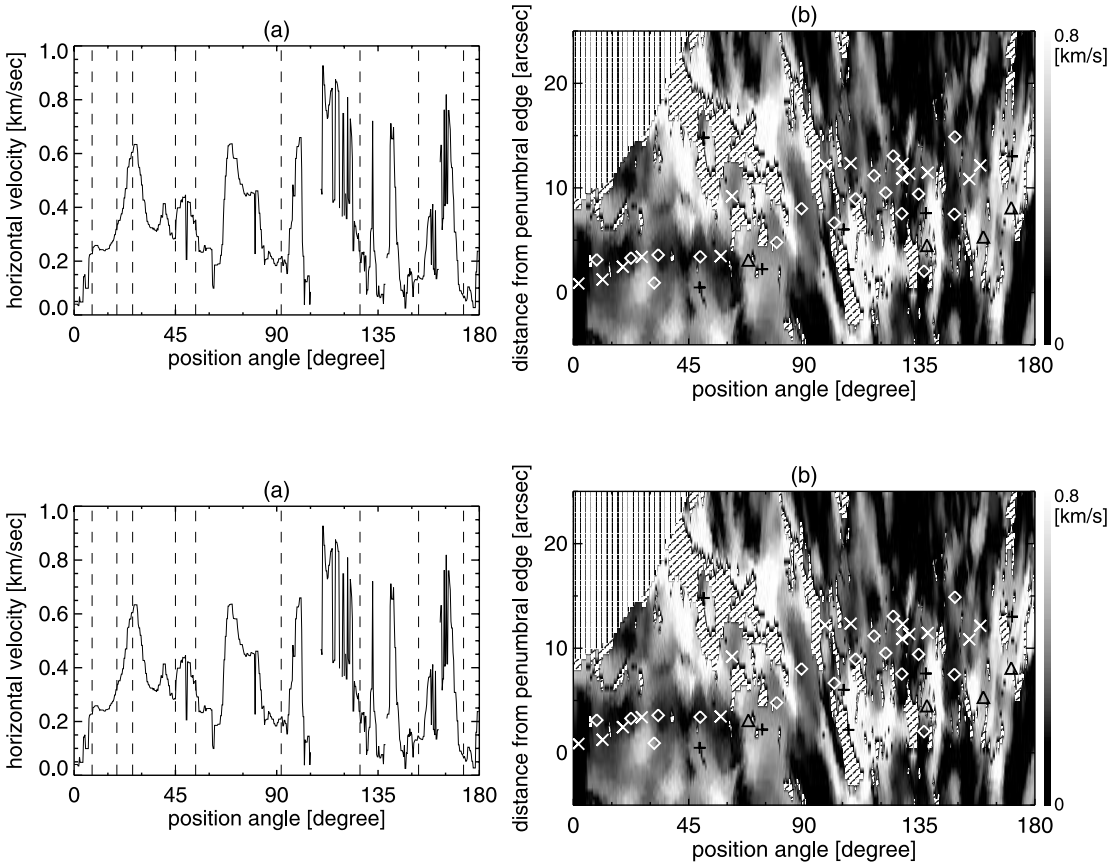

FIG. 8.—(*a*) Variation of horizontal velocity v_h obtained with the local correlation technique for the MDI line-of-sight magnetic signal along the penumbral outer boundary. The vertical dashed-lines correspond to spines of the penumbra. (*b*) Horizontal velocity for the moat region in the radial distance (d_p) from the penumbral outer boundary-position angle (ψ_p)-plane. The triangles and diamonds show positions of the positive-polarity isolated MMFs with high horizontal velocity ($v_h > 0.4$ km s^{-1}) and small horizontal velocity ($v_h < 0.4$ km s^{-1}), respectively. The plus and cross symbols show positions of the negative-polarity isolated MMFs with high horizontal velocity ($v_h > 0.4$ km s^{-1}) and small horizontal velocity ($v_h < 0.4$ km s^{-1}), respectively. The hatched areas with vertical lines represent areas out of the ASP field of view. The hatched areas with oblique lines represent invalid MDI data areas, which have magnetic flux less than 10 G or the maximum correlation coefficient less than 0.9. (*c*) Same as panel *a* for Doppler velocity v_{los} obtained with the ASP Stokes profiles. (*d*) Same as panel *b* for the unsigned Doppler velocity. The contours represent the horizontal velocity of 0.7 km s^{-1}. The hatched areas with oblique lines represent areas where degree of polarization is less than 0.4%. [*See the electronic edition of the Journal for a color version of this figure.*]

TABLE 1

COMPARISON BETWEEN ISOLATED AND NONISOLATED MMFS

Penumbral Field	Evershed Flow	Polarity to Sunspot	Inclination	Horizontal Velocity	Location in Moat
		Isolated MMFs			
Vertical	No	Same	Vertical	Low	Middle–outer
Horizontal.....	Yes	Both	Horizontal	High	Inner–middle
	Yes	Both	Horizontal	Low	Middle–outer
	Yes	Opposite	Vertical	Low	Outer
		Nonisolated MMFs			
Horizontal.....	Yes	Inner: same/outer: opposite	Horizontl	High	Inner–middle
	No	Inner: same/outer: opposite	Horizontal	Low	Middle–outer
Veritical	No	Inner: same/outer: opposite	Horizontal	Low	Middle–outer

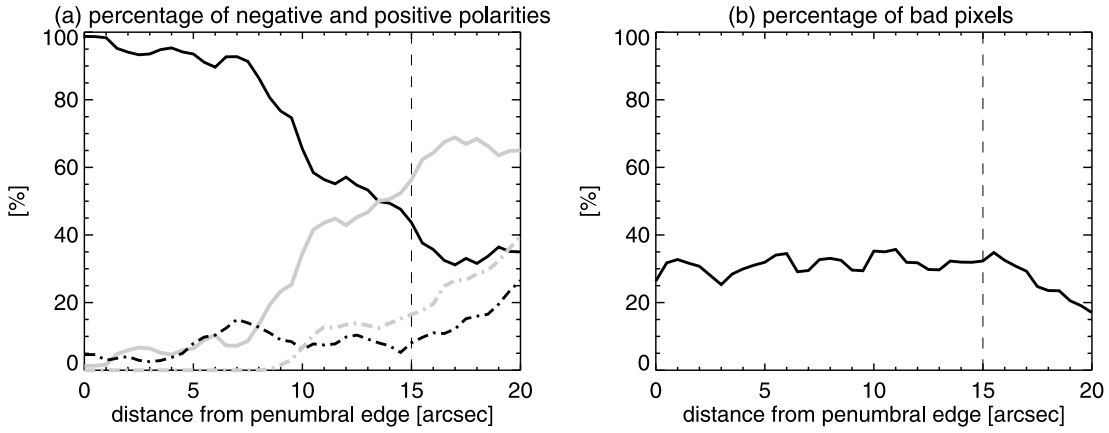

FIG. 9.—(*a*) Percentage of pixels with positive and negative polarities obtained with the ASP as functions of distance (d_p) from the penumbral outer boundary. (*b*) Percentage of bad pixels. Both are for the position angle ψ_p of 60°–180°. The vertical axis represents the normalized number of pixels. The black and gray solid lines in panel *a* represent pixels with positive and negative polarities, respectively. The black and gray dash-dotted lines represent pixels having vertical magnetic fields with positive (α) and negative ($135^\circ < \gamma < 180^\circ$) polarities, respectively. See § 4.1 for the bad pixels.

magnetic fields appear to be subset of the nonisolated MMFs, and have magnetic fields slightly inclined with respect to magnetic fields of the nonisolated MMFs (see Fig. 2).

5. TRANSPORT OF MAGNETIC FLUX BY MMFs

5.1. *Radial Variation in Flux Transport Rate of MMFs*

In this section we obtain the variation of number, horizontal velocity, and flux transport rate for all the MMFs, as well as for only MMFs with vertical magnetic fields ($0^\circ < \gamma < 45^\circ$ and $135^\circ < \gamma < 180^\circ$) as functions of distance (d_p) from the penumbral outer boundary. All the MMFs contain both the isolated and nonisolated MMFs. The MMFs with vertical magnetic fields almost correspond to the isolated MMFs with vertical magnetic fields (see Table 1).

5.1.1. *Number of MMFs with Positive and Negative Polarities*

Figure 9*a* shows the percentage of pixels with positive and negative polarities for position angle ψ_p of 60°–180° at different radial distance (d_p). The variation in the percentage of pixels is not due to the bad pixels (see § 4.1), since the percentage of the bad pixels is almost constant at any distance (Fig. 9*b*).

The area near the outer penumbral boundary ($d_p < 7''$) is occupied by MMFs with positive polarity. The percentage of the MMFs with positive polarity decreases beyond $d_p = 7''$, while the percentage of the MMFs with negative polarity increases. The percentage of MMFs with positive and negative polarities is nearly same in the outer area of the moat region ($d_p = 10''$–$15''$).

The gray dash-dotted line shows that the percentage of the negative-polarity MMFs with vertical magnetic fields ($135^\circ < \gamma < 180^\circ$) increases from 0% to about 15% around $d_p = 10''$. This corresponds to the location of the isolated MMFs having vertical magnetic fields with negative polarity (see Table 1). The percentage of the positive-polarity MMFs with vertical magnetic fields ($0^\circ < \gamma < 45^\circ$) does not increase around $d_p = 10''$ like the negative-polarity MMFs with vertical magnetic fields. Variation in the percentage of the vertical positive-polarity MMFs does not coincide with that of the vertical negative-polarity MMFs. The percentage of the vertical positive-polarity MMFs increases just outside the penumbral spines ($d_p \sim 5''$). The MMFs located there have inclinations of 0°–45°, while the spines have typical inclinations of 50°–70°.

5.1.2. *Horizontal Velocity*

Radial outward velocity gradually becomes slower with increasing distance (d_p) from the outer boundary of the penumbra for both positive (Fig. 10*a*, *black solid line*) and negative (*gray solid line*) polarities. The radial outward velocity for negative polarity has a peak around $d_p = 5''$. This corresponds to the location of high horizontal velocity channels. The radial outward velocity for the positive-polarity MMFs with vertical magnetic fields (*black dash-dotted line*) is nearly zero within $5''$ from the penumbral outer boundary. Thus, the penumbral spines, which extend up to around $d_p = 5''$, have no apparent radial motion. The radial outward velocity for the positive-polarity MMFs with vertical magnetic fields is about 0.2 km s^{-1}, which is slower than other features in the moat region outside the spines ($d_p = 5''$–$15''$).

5.1.3. *Flux Transport Rate*

We estimate the radial transport rate of MMFs for position angles ψ_p of 60°–180° as $\Phi_r = \int_{\psi_p=60}^{\psi_p=180} (f|\boldsymbol{B}| \cos\gamma) v_r r d\psi_p$, where f is filling factor, $|\boldsymbol{B}|$ is field strength, γ is inclination of magnetic fields to the local vertical, v_r is radial component of horizontal velocity, and ψ_p is the position angle. The magnetic parameters ($|\boldsymbol{B}|$, f, and γ) are obtained from the ASP, and the horizontal velocity is obtained with the local correlation technique from the MDI line-of-sight magnetic signal. The size of one ASP pixel ($0.37''$) is used for $dl = r d\psi_p$. Figure 10*b* show that the radial transport rate of the MMFs with positive polarity (*black solid line*) decreases for $d_p = 7''$–$10''$, while the radial transport rate of the MMFs with negative polarity (*gray solid line*) increases for the same distance. This change in the radial transport rate for $d_p = 7''$–$10''$ is mainly due to the change in the number of positive and negative polarities (see Fig. 9*a*). Most of magnetic flux with negative polarity is carried by the MMFs with vertical magnetic fields (*gray dash-dotted line*). The radial transport rate of the positive-polarity MMFs with vertical magnetic fields (*black dash-dotted line*) increases just outside the penumbral spines ($d_p \sim 5''$).

The radial transport of positive flux decreases by a factor of 10 from $d = 3''$–$15''$, while a large increase of the negative flux transport occurs at $d = 7''$. These large variations suggest that the solid lines of Figure 10*b* do not represent only the real transport of flux, but also flux emergence and cancellation in the moat region. It is also possible that only a small fraction of the flux considered in the calculations is actually flowing radially outward. This would be

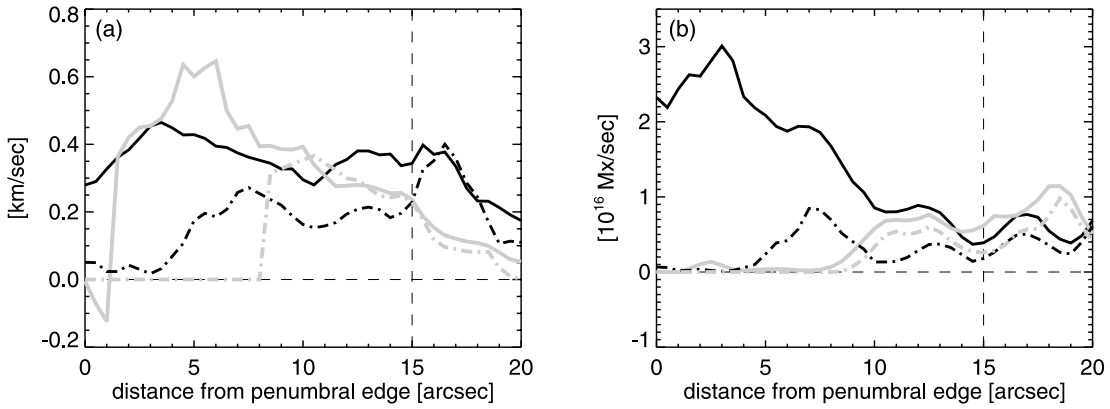

FIG. 10.—(*a*) Variations in the radial component of horizontal velocity and (*b*) the radial transport rate of MMFs as functions of distance (d_p) from the penumbral edge. The horizontal velocity is obtained with the local correlation technique for the MDI line-of-sight magnetic signal, and it is averaged for position angle ψ_p of 60°–180°, excluding the bad pixels (see § 4.1). See the text for the method of calculating the radial transport rate. The black and gray solid lines represent pixels with positive and negative polarities, respectively. The black and gray dash-dotted lines represent pixels having vertical magnetic fields with positive ($0° < \gamma < 45°$) and negative ($135° < \gamma < 180°$) polarities, respectively. Radial outward velocity and transport are positive.

the case if the radial velocity derived from the MDI magnetograms does not correspond to a real outward motion, but only to the propagation velocity of a local fluctuation. These considerations should be kept in mind for the rest of this section.

5.2. *Comparison between Flux Transport by MMFs and Flux Loss of Sunspots*

The magnetic flux (positive polarity) of the sunspot decreases at a rate of about $(0.7–0.8) \times 10^{21}$ Mx day^{-1} during March 12–14, as shown in Figure 11. We compare this flux loss rate of the sunspot with the flux transport rate of MMFs (Table 2).

5.2.1. *Flux Transport Rate of All MMFs*

MMFs separate completely from the penumbral uncombed structure around the middle of the moat region ($d_p = 7''$). Thus, the radial outward flux transport rate at $d_p = 7''$ corresponds to magnetic flux carried away from the sunspot. Most of the MMFs have positive polarity around $d_p = 7''$. The flux transport rate of the positive-polarity MMFs (5.0×10^{21} Mx day^{-1}) is much larger than that of the negative-polarity MMFs (0.1×10^{21} Mx day^{-1}), and is about 7 times larger than the flux loss rate of the sunspot. Total magnetic flux of the sunspot is about 2×10^{22} Mx on March 12. If MMFs carry away magnetic flux from the sunspot with the constant rate of 5.0×10^{21} Mx day^{-1}, the sunspot would have completely disappeared within 4 days.

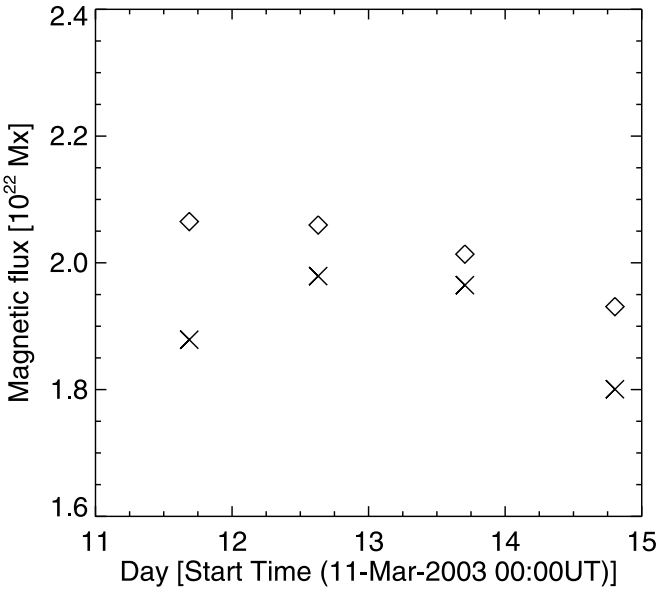

FIG. 11.—Time profile of magnetic flux (positive polarity) for the sunspot in NOAA 10306 during 2003 March 11–14. The magnetic flux is derived from the ASP magnetic flux map. The outer edge of the sunspot is determined from the continuum intensity as explained in § 4.1. The crosses show the observed magnetic flux. The diamonds show magnetic flux corrected for the projection effect due to the location on the solar disk.

Martínez Pillet (2002) estimated that the rate of flux generation by appearance of MMFs with polarity same as the sunspots $[(3.5–5.1) \times 10^{20}$ Mx day$^{-1}]$ was 3–8 times larger than the flux loss rate of the sunspots $[(0.6–1.44) \times 10^{20}$ Mx day$^{-1}]$ for two mature sunspots observed with the ASP during several days. Our result is consistent with the result of Martínez Pillet (2002), although our estimated flux transport rate $[(2.3–5.0) \times 10^{21}$ Mx day$^{-1}]$ is 1 order of magnitude larger than the flux generation rate estimated by Martínez Pillet (2002). The larger value may be due to the size of our sunspot, whose radius is about 2–3 times larger than those of the two sunspots studied by Martínez Pillet (2002).

5.2.2. *Flux Transport Rate of MMFs with Vertical and Horizontal Magnetic Fields*

The fact that the flux transport rate of MMFs is larger than the flux loss rate of the sunspot near the penumbra indicates that only a limited part of the MMFs contributes to the flux loss of the sunspot. The flux transport rates of the positive-polarity MMFs with vertical and horizontal magnetic fields are 3–4 times larger than the flux loss rate of the sunspot at $d_p = 7''$. Thus, the vertical and horizontal MMFs can carry away sufficient magnetic flux for the flux loss of the sunspot.

The flux transport rate of the vertical MMFs should be more important in terms of the decay of the sunspot, because it is possible that the horizontal MMFs correspond to the propagation of a local fluctuation of the magnetic field. The vertical positive-polarity MMFs do not occupy all over the moat region on the lines extrapolated from the penumbral spines. Thus, it is appropriate that their flux transport rate is averaged over $d_p = 7–15''$ (Fig. 10*b*). The averaged flux transport rate (0.9×10^{21} Mx day^{-1}) is nearly equal to the flux loss rate of the sunspot. If the vertical positive-polarity MMFs alone contribute to the flux loss of the sunspot,

TABLE 2
Summary of Flux Transport Rate of MMFs

Parameter	Positive[a]			Negative[a]		
	Vertical	Horizontal	Total	Vertical	Horizontal	tTotal
			$d_p = 7''$			
Area (%).....	15	78	93	0	7	7
Φ_r (10^{21} Mx day^{-1}).....	2.2	2.8	5.0	0.0	0.1	0.1
			$d_p = 12''$			
Area (%).....	10	47	57	13	30	43
Φ_r (10^{21} Mx day^{-1}).....	0.7	1.6	2.3	1.4	0.4	1.8
			Average d_p ($7''$–$15''$)			
Area (%).....	9	55	64	9	27	36
Φ_r (10^{21} Mx day^{-1}).....	0.9	1.7	2.6	0.8	0.4	1.2

Notes.—The value d_p is the distance from the penumbral outer boundary. The radial transport rate, Φ_r, is integrated in the entire azimuth angle (360°).
[a] Sunspot polarity.

the disintegration of the sunspot can be explained without inconsistency.

6. DISCUSSION

6.1. *Magnetic Correspondence between MMFs and Penumbra*

We extend the definition of MMFs to cover not only the classical MMFs (isolated MMFs) but also any moving magnetic fields in the moat (nonisolated MMFs). We find significant magnetic correspondence between the isolated MMFs and the uncombed structure of the sunspot penumbra. This correspondence is summarized as follows (see also Table 1 and Fig. 12):

1. The magnetic fields of the isolated MMFs located on the lines extrapolated from the spine, which is the vertical component of the penumbral uncombed structure, are more vertical to the solar surface than the surroundings. The magnetic fields of these MMFs are more vertical than the penumbral spines. These MMFs have polarity same as the sunspot. Their horizontal velocities are slower than those of the other MMFs.
2. The isolated MMFs with nearly horizontal magnetic fields are located on the lines extrapolated from the horizontal component of the penumbral uncombed structure. They have both polarities. Their horizontal velocities are higher near the penumbra on the lines extrapolated from the Evershed channels, which are located in the horizontal component of the uncombed structure.
3. There are some isolated MMFs with vertical magnetic fields located on the lines extrapolated from the horizontal component of the penumbral uncombed structure. They are only located around the outer boundary of the moat region, and have polarity opposite to the sunspot.

The isolated MMFs located on the lines extrapolated from the vertical component of the penumbral uncombed structure correspond to the type II MMFs. The isolated MMFs with horizontal magnetic fields have properties similar to the nonisolated MMFs in terms of magnetic fields and horizontal velocities. The moat region on the lines extrapolated from the horizontal component of the uncombed structure is occupied by nonisolated and isolated MMFs having nearly horizontal magnetic fields with both polarities. Thomas et al. (2002b) and Weiss et al. (2004) have proposed that type II MMFs are formed as a result of the detachment of the vertical component of the penumbral uncombed structure are detached from sunspots (Fig. 12*b*, *top panel*), while type I and type III MMFs correspond to intersections of the horizontal fields extended from the penumbra (Fig. 12*b*, *bottom panel*). Our observation on the magnetic correspondence between the isolated MMFs and the penumbral magnetic fields, for the first time, suggests that this interpretation is correct. The magnetic field structures on the lines extrapolated from the horizontal component of the uncombed structure can be interpreted as the shape of a sea serpent (Harvey & Harvey 1973; Schlichenmaier 2002). The type II MMFs contribute to the disintegration of the sunspot. We find their flux transport rate is about 1–3 times larger than the flux loss rate of the sunspot. Therefore, we conclude that the type II MMFs alone can carry away sufficient magnetic flux, so that they could be responsible for the decay of the sunspot.

The magnetic flux transported by all MMFs is much larger than the flux loss rate of the sunspot. A possible way out of the problem is that only some MMFs are actually responsible for the sunspot decay. Indeed, it has been suggested that only type II MMFs contribute to the flux loss of sunspots, while type I (bipolar) MMFs would not contribute because they represent the propagation of a local perturbation of horizontal field lines (e.g., Shine & Title 2001; Martínez Pillet 2002; Thomas et al. 2002b; Weiss et al. 2004). MMFs that do not carry magnetic flux away from the spot must appear as pairs of opposite polarities. Our observations do not show clear bipolar MMFs, and so the number of MMFs with positive polarity is much larger than the number of negative-polarity MMFs near the penumbra. It may well be possible that this excess of positive-polarity MMFs is due to bipolar MMFs whose negative-polarity elements are not detected. This could explain (part of) the large imbalance between the sunspot flux loss rate and the flux transport rate of MMFs. In the next section, we discuss possible reasons why clear MMFs pairs are not present in our data.

6.2. *Bipolar MMFs and Unipolar MMFs*

Bipolar MMFs (type I MMF) tend to appear in positions at dark penumbral filaments with horizontal magnetic fields (Lee 1992; Ryutova et al. 1998; Shine & Title 2001), and the majority of MMF pairs first appear at $2''$–$7''$ from the outer penumbral boundary

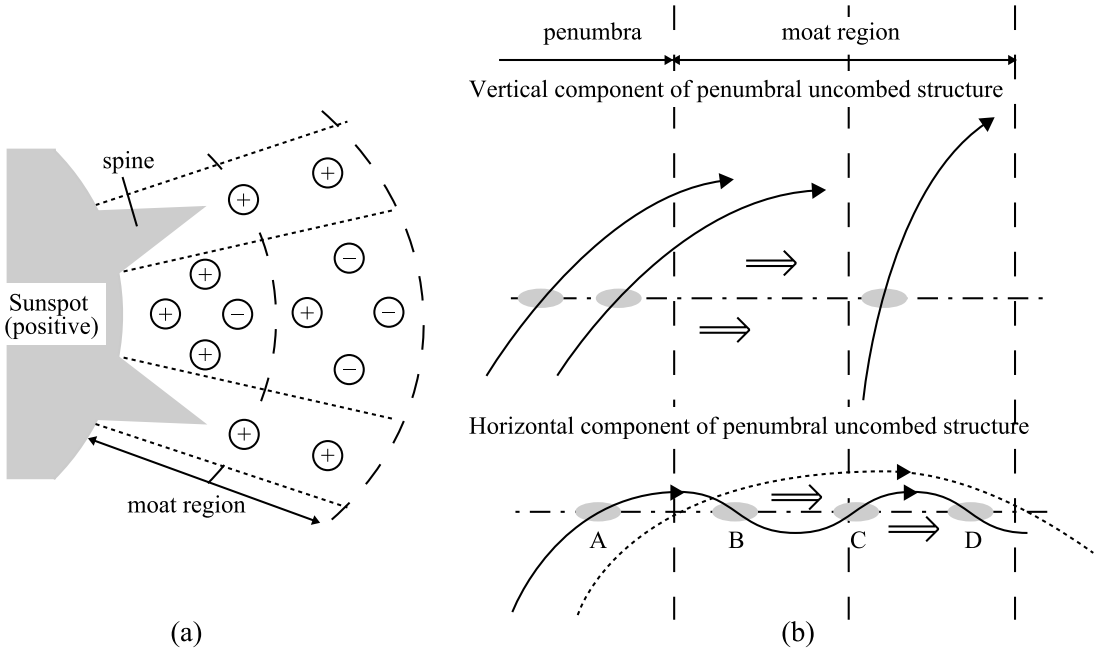

FIG. 12.—Schematic illustrations of the spatial distribution of (*a*) MMFs with positive and negative polarities in the moat region, and (*b*) of the magnetic field structures of MMFs and the penumbral uncombed structure. The black solid lines represent magnetic field lines whose footpoints are located on the line extrapolated from the vertical component of the penumbral uncombed structure in top panel and magnetic field lines whose footpoints are located on the line extrapolated from the horizontal component in bottom panel. The dotted line represents the averaged magnetic field of the nonisolated MMFs. The horizontal dash-dotted line represents the photospheric surface. The intersections of the black solid line with the photosphere are represented by A, B, C, and D in the bottom panel.

(Zhang et al. 2003). It has been suggested that bipolar MMFs are the intersection of a convex (Harvey & Harvey 1973; Nye et al. 1984; Ryutova et al. 1998; Shine & Title 2001; Thomas et al. 2002b) or a concave (Zhang et al. 2003) part of horizontal magnetic field in the moat region. However, we do not obtain clear MMF pairs in our data. Zhang et al. (2003) identified clear 144 MMF pairs from about 88 hr sequence of the MDI magnetograms in the high-resolution mode. Martínez Pillet (2002) estimated five bipolar MMFs per hour. The single ASP map covers only about 50% of the moat region, and requires 20 minutes to be completed. According to the rate of appearance of bipolar MMFs in Zhang et al. (2003) and Martínez Pillet (2002), we expect to see $144/88/3 \times 0.5 = 0.3$ bipolar MMFs or $5/3 \times 0.5 = 0.8$ bipolar MMFs in this particular ASP map. This result is consistent with no identification of clear bipolar MMFs in our observation. Hagenaar & Shine (2005) also obtained only single-polarity MMFs and did not obtain bipolar MMFs for about 2000 MMFs around eight sunspots observed with the high-resolution mode of the MDI. It is difficult to identify a pair of bipolar MMFs, especially MMFs with horizontal magnetic fields, because of the following two reasons.

One is that the detection of MMFs may be influenced by ambient magnetic fields due to the lack of spatial resolution. When a pair of isolated MMFs is mixed with the ambient magnetic fields of the nonisolated MMFs, as shown in Figure 13, the isolated MMF with negative polarity, which is opposite to polarity of the ambient magnetic fields, has smaller magnetic flux and is not detectable as a result. Previous observations frequently show such an imbalance of the magnetic flux and the size of MMF pairs (Ryutova et al. 1998; Yurchyshyn et al. 2001; Zhang et al. 2003). On the other hand, the isolated MMF with positive polarity may not be distinguished from the ambient magnetic fields if magnetic field inclination of the isolated MMF is similar to that of the ambient magnetic fields. In this case, only the MMF with negative polarity is identified. When the nonisolated MMFs consist of small-scale bipolar MMFs and ambient magnetic fields without horizontal motion, the small-scale bipolar MMFs are influenced by the ambient fields in the same way. The flux transport rate of the horizontal positive-polarity MMFs is much larger than that of the negative-polarity MMFs near the penumbra as a result. The same result is obtained for U-shaped MMFs.

Another reason is that one footpoint of a MMF pair is located in the sunspot and the other footpoint moves outward such as intersections A and B in Figure 12*b*. In this case, only the MMF with negative polarity, which is opposite to the polarity of the sunspot, is observed. The isolated vertical negative-polarity MMFs located around the outer boundary of the moat region also have a unipolar structure. The number of the vertical negative-polarity MMFs increases in the outer area of the moat region, while increase in the number of the vertical positive-polarity MMFs is not observed (Fig. 9*a*). This cannot be explained by the influence of the ambient magnetic fields. Therefore, we propose that positive-polarity elements associated with the vertical negative-polarity MMFs are located in the sunspot. The origin and formation process of the vertical negative-polarity MMFs still remain open issues.

The magnetic field structures on the lines extrapolated from the horizontal component of the penumbral uncombed structure would not always form the shape of clear sea serpents as shown

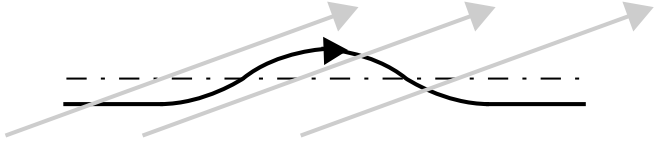

FIG. 13.—Horizontal MMF pair is mixed with ambient magnetic fields (*gray lines*) in the moat region. The dash-dotted line represents the photospheric surface. This illustration shows an Ω-shaped MMF.

in the bottom panel of Figure 12*b*. Whether clear MMFs pairs are formed depends on ambient magnetic fields around them or their relationship to the penumbral magnetic fields.

7. CONCLUSIONS

We have obtained the magnetic properties and horizontal motions of isolated and nonisolated MMFs. The nonisolated MMFs occupy most of the moat region surrounding the isolated MMFs, and have nearly horizontal magnetic fields with both polarities. The isolated MMFs with horizontal magnetic fields have similar magnetic properties as the nonisolated MMFs.

We find that isolated MMFs have magnetic correspondence to the uncombed structure of the sunspot penumbra. The moat region on the lines extrapolated from the horizontal component of the penumbral uncombed structure is occupied by horizontal isolated MMFs and the nonisolated MMFs with both polarities. This suggests that these MMFs correspond to part of horizontal field lines extending from the penumbra and forming the shape of a sea serpent. The isolated MMFs located on the lines extrapolated from the vertical component of the penumbral uncombed structure always have magnetic fields vertical to the solar surface and polarity same as the sunspot. This shows that these MMFs are formed when the vertical component of the uncombed structure is detached from the penumbra. We estimate that the magnetic flux carried away from the sunspot by these MMFs is 1–3 times larger than flux loss rate of the sunspot. If all MMFs carry magnetic flux away from the sunspot, their flux transport rate is about 7 times larger than the flux loss rate of the sunspot just outside the penumbra. We conclude that only the vertical isolated MMFs with polarity same as the sunspot are responsible for the disintegration of the sunspot.

A clear relationship between the horizontal motion of MMFs and the Evershed flows, which are located in the horizontal component of the penumbral uncombed structure, is observed. We find that both the isolated and nonisolated MMFs have higher horizontal velocity (>0.4 km s^{-1}) on the lines extrapolated from the Evershed flow channels. The mechanism by which the Evershed flows drive motion of the MMFs still remains an open issue.

In this paper we have focused on MMFs around a regular decaying sunspot. It is necessary for the understanding of the decaying process of sunspots in general to confirm whether the magnetic correspondence between MMFs and the penumbra is common to other sunspots.

We gratefully acknowledge the helpful comments and suggestions of an anonymous referee. We are also grateful to Y. Katsukawa, Y. Sakamoto, and K. Ichimoto for useful discussions on this paper. We thank the US National Solar Observatory and the HAO for the setup and operation of the ASP. T. Tarbell is acknowledged for supporting the observations of *TRACE* and *SOHO*, and for helping the authors to polish the manuscript. The coordinated observations were carried out by the JSPS Japan-US science program "Collaborative research of solar explosive phenomena with *Yohkoh*/*SOHO*/*TRACE*/*Solar-B*."

APPENDIX

CORONAL ACTIVITIES AROUND THE SUNSPOT

This section describes coronal activities observed with *TRACE* 171 Å images around the sunspot. X-ray observations have revealed that transient coronal phenomena such as microflares (Shimizu 1994; Shimizu et al. 2002), flares (Yurchyshyn & Wang 2001), X-ray jets and surges (Wang et al. 1991; Shimojo et al. 1996; Canfield et al. 1996) occur preferentially around magnetic flux concentrations located near the outer boundary of the moat region. There are reports showing that coronal transient activities occur at locations where MMFs cancel with a flux concentration (Wang et al. 1991; Yurchyshyn & Wang 2001).

Figure 14*a* shows that flux concentrations with negative polarity (*black regions; small spots are seen in continuum*) are observed for 4 days outside the moat region. Coronal steady bright structures (Fig. 14*b*, *black*) are always observed above the flux concentrations. These bright structures are called moss, which is fiducial for the footpoints of the hot loops with temperature higher than 3 MK (Berger et al. 1999; Martens et al. 2000; Katsukawa & Tsuneta 2005). Some transient bright loops appear to connect the moss region to the outer part of the sunspot penumbra. These loops are shorter and more inclined than the fanlike loops seen around the southwest of the sunspot. The steady fanlike loops connect positive polarity of the sunspot with negative polarity located in the following plage region (out of the panels). Figure 14*a* shows that a few elongated and enhanced spine structures are located in the moat region between the flux concentrations and the sunspot. Clear examples are observed on March 11 and 14. These enhanced structures have more vertical magnetic fields than other spines (see Fig. 4*a*). The transient bright loops connecting the moss region and the penumbra are observed around the enhanced spine structures. One of them is shown by a gray arrow in top panel of Figure 14*b*.

There is no apparent bright structure associated with MMFs in the moat region. Some transient brightenings are observed around the outer boundary of the moat region. One of these transient brightenings is shown by a black arrow in Figure 14*b*. A pair of MMFs is located beneath this bright structure (Fig. 15, *white arrows*). It is not clear when they appeared, because MDI magnetograms are available only every 96 minutes in the non-ASP observing period. They simultaneously become larger in size from about 14 : 30 UT around the outer boundary of the moat region, and then they separate from each other (Fig. 16*a*). The MMF with negative polarity merges into the flux concentration located north of the MMF, while the MMF with positive polarity collides with another negative MMF located south of the positive MMF (Fig. 16*b*). The positive MMF disappears with occurrence of two coronal brightenings at 22 : 19 and 22 : 49 UT (22 : 19 UT frame in Figs. 15 and 16*c*). The duration of the brightenings is about 15 minutes. The brightenings are probably the result of magnetic reconnection between magnetic field lines of the colliding opposite polarity MMFs.

An area with blueshift of about 0.3 km s^{-1} is distributed along the outer boundary of the moat region as shown by arrows in Figure 17*a*. The sunspot is located near disk center and magnetic fields of the moat region are nearly horizontal to the solar surface. If we interpret the observed blueshift to be emergence of horizontal magnetic fields, small-scale flux emergence, which cannot be resolved in our observations, frequently occurs around the outer boundary of the moat region. Such small-scale flux emergence and magnetic flux cancellation around the outer boundary of the moat region would drive these transient brightenings.

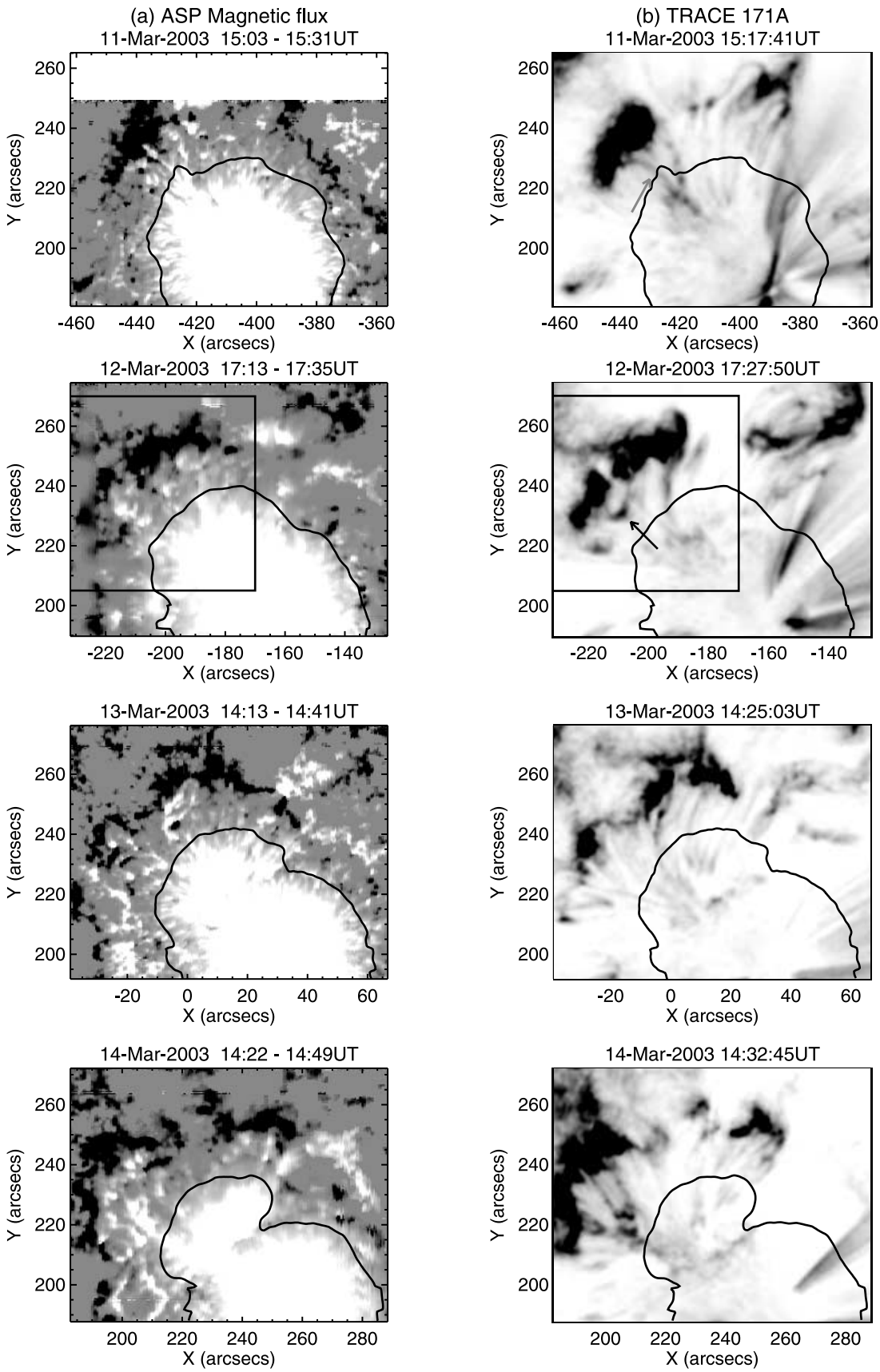

FIG. 14.—(*a*) Day-by-day changes of ASP magnetic flux and (*b*) *TRACE* 171 Å coronal images (negative prints) around the sunspot in active region NOAA 10306 from March 11 to 14. White (black) is positive (negative) polarity in panel *a*. Coronal bright features are displayed in black in panel *b*. The solid boxes delineate the field of view for Figs. 15 and 17. The black line represents the outer boundary of the penumbra. See the text for arrows in the panels.

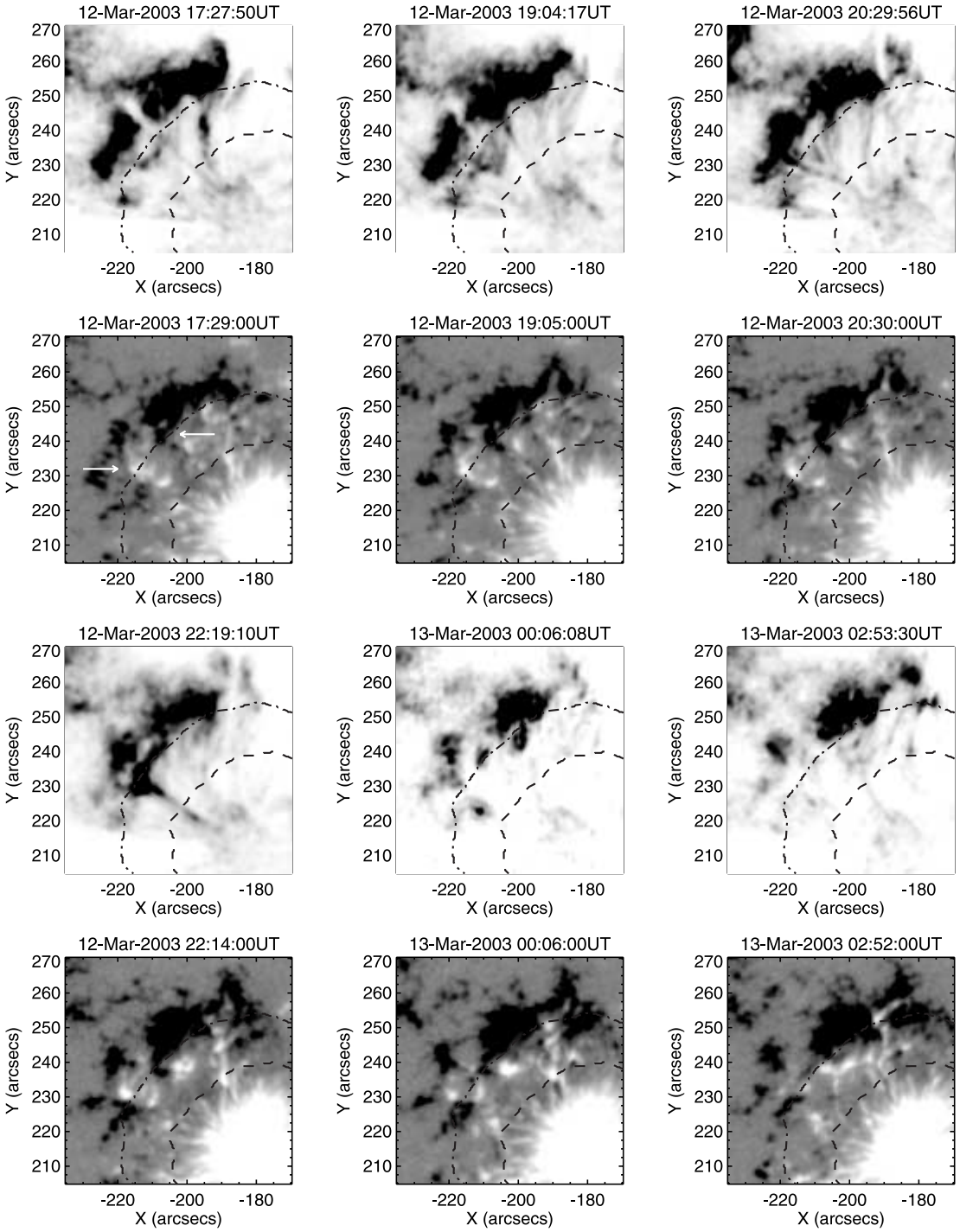

FIG. 15.—Transient brightenings associated with MMFs on March 12–13. The field of view of panels is identical to the box in Fig. 14. Coronal images are *TRACE* 171 Å. Coronal bright features are displayed in black. Longitudinal magnetograms are obtained with the high-resolution mode of the MDI. White shows positive polarity, and black shows negative polarity. The white arrows indicate a pair of MMFs. The dashed and dash-dotted lines represent the outer boundary of the penumbra and the position of 15″ away from the penumbral outer boundary. These lines are determined from the ASP data taken in 17 : 13–17 : 35 UT on 2003 March 12.

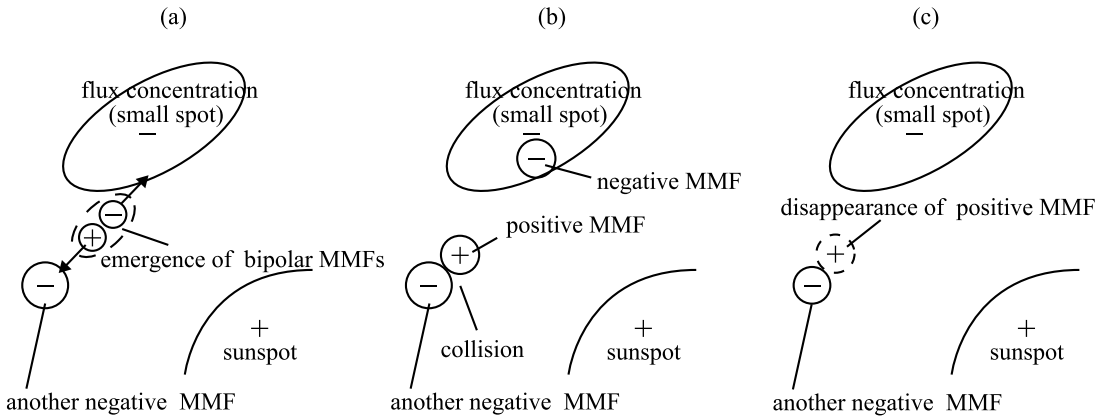

FIG. 16.—Illustration for temporal changes in the pair of MMFs shown by the white arrows in Fig. 15.

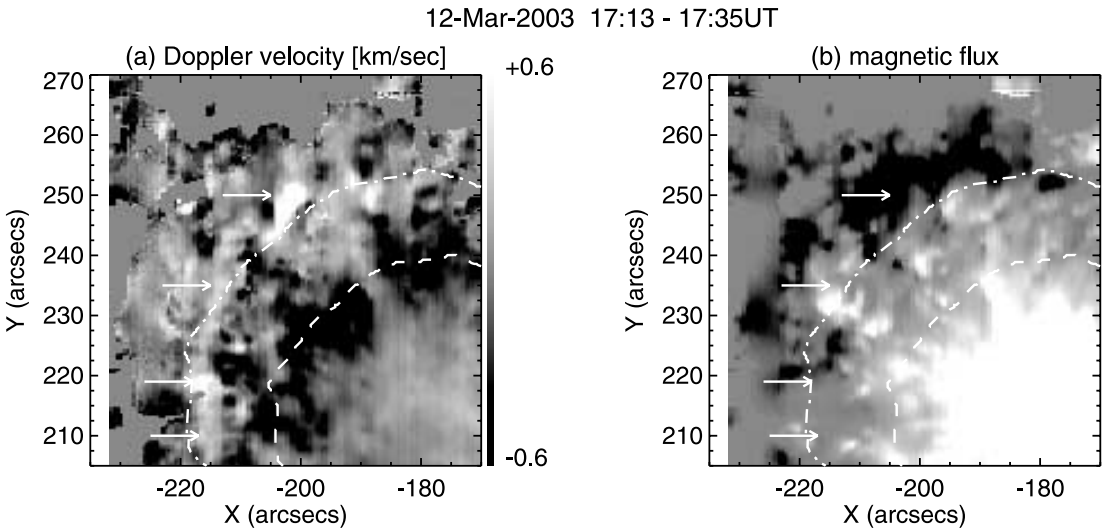

FIG. 17.—(*a*) Doppler velocity and (*b*) magnetic flux map obtained with the ASP on 2003 March 12. The field of view of the panels is identical to the box in Fig. 14. Positive velocity (white) corresponds to blueshift in panel *a*, and white (black) is for positive (negative) polarity in panel *b*. The dashed line represents the outer boundary of the penumbra. The dash-dotted line shows the position of 15″ away from the penumbral outer boundary. The arrows show areas with blueshift located along the outer boundary of the moat region.

REFERENCES

Bellot Rubio, L. R., Balthasar, H., & Collados, M. 2004, A&A, 427, 319
Bellot Rubio, L. R., Balthasar, H., Collados, M., & Schlichenmaier, R. 2003, A&A, 403, L47
Berger, T. E., De Pontieu, B., Fletcher, L., Schrijver, C. J., Tarbell, T. D., & Title, A. M. 1999, Sol. Phys., 190, 409
Brickhouse, N. S., & Labonte, B. J. 1988, Sol. Phys., 115, 43
Bonet, J. A., Márquez, I., Muller, R., Sobotka, M., & Tritschler, A. 2004, A&A, 423, 737
Borrero, J. M., Lagg, A., Solanki, S. K., & Collados, M. 2005, A&A, 436, 333
Borrero, J. M., Solanki, S. K., Bellot Rubio, L. R., Lagg, A., & Mathew, S. K. 2004, A&A, 422, 1093
Cabrera Solana, D., Bellot Rubio, L. R., Beck, C., & del Toro Iniesta, J. C. 2006, ApJ, 649, L41
Canfield, R. C., Reardon, K. P., Leka, K. D., Shibata, K., Yokoyama, T., & Shimojo, M. 1996, ApJ, 464, 1016
Chae, J., Wang, H., Qiu, J., Goode, P. R., Strous, L., & Yun, H. S. 2001, ApJ, 560, 476
Degenhardt, D., & Wiehr, E. 1991, A&A, 252, 821
Domingo, V., Fleck, B., & Poland, A. I. 1995, Sol. Phys., 162, 1
Elmore, D. F., et al. 1992, Proc. SPIE, 1746, 22
Hagenaar, H. J., & Shine, R. A. 2005, ApJ, 635, 659
Handy, B. N., et al. 1999, Sol. Phys., 187, 229
Harvey, K., & Harvey, J. 1973, Sol. Phys., 28, 61
Katsukawa, Y., & Tsuneta, S. 2005, ApJ, 621, 498
Krivova, N. A., & Solanki, S. K. 2004, A&A, 417, 1125
Kubo, M., Shimizu, T., & Lites, B. W. 2003, ApJ, 595, 465
Lee, J. W. 1992, Sol. Phys., 139, 267
Lites, B. W., Elmore, D. F., Seagraves, P., & Skumanich, A. P. 1993, ApJ, 418, 928
Lites, B. W., Low, B. C., Martinez Pillet, V., Seagraves, P., Skumanich, A., Frank, Z. A., Shine, R. A., & Tsuneta, S. 1995, ApJ, 446, 877
Lites, B. W., & Skumanich, A. 1990, ApJ, 348, 747
Martens, P. C. H., Kankelborg, C. C., & Berger, T. E. 2000, ApJ, 537, 471
Martínez Pillet, V. 2002, Astron. Nachr., 323, 342
Mathew, S. K., Lagg, A., Collados, M., Borrero, J. M., Berdyugina, S., Krupp, N., Woch, J., & Frutiger, C. 2003, A&A, 410, 695
November, L. J., & Simon, G. W. 1988, ApJ, 333, 427
Nye, A. H., Thomas, J. H., & Cram, L. E. 1984, ApJ, 285, 381
Rimmele, T. R. 1995, ApJ, 445, 511
Ryutova, M., Shine, R., Title, A., & Sakai, J. I. 1998, ApJ, 492, 402
Sainz Dalda, A., & Martínez Pillet, V. 2005, ApJ, 632, 1176
Sakamoto, Y. 2004, in ASP Conf. Ser. 325, The *Solar-B* Mission and the Forefront of Solar Physics, ed. T. Sakurai & T. Sekii (San Francisco: ASP), 151
Scherrer, P. H., et al. 1995, Sol. Phys., 162, 129
Schlichenmaier, R. 2002, Astron. Nachr., 323, 303
Shimizu, T. 1994, in Proc. Kofu Symposium, ed. S. Enome & T. Hirayama (Nagano: Nobeyama Radio Obs.), 61
Shimizu, T., Shine, R. A., Title, A. M., Tarbell, T. D., & Frank, Z. 2002, ApJ, 574, 1074
Shimojo, M., Hashimoto, S., Shibata, K., Hirayama, T., Hudson, H. S., & Acton, L. W. 1996, PASJ, 48, 123
Shine, R., & Title, A. 2001, Encyclopedia of Astronomy and Astrophysics, Vol. 4, ed. P. Murdin (Bristol: IOP), 3209
Skumanich, A., & Lites, B. W. 1987, ApJ, 322, 473
Stanchfield, D. C. H., Thomas, J. H., & Lites, B. W. 1997, ApJ, 477, 485
Title, A. M., Frank, Z. A., Shine, R. A., Tarbell, T. D., Topka, K. P., Scharmer, G., & Schmidt, W. 1993, ApJ, 403, 780
Thomas, J. H., Weiss, N. O., Tobias, S. M., & Brummell, N. H. 2002a, Astron. Nachr., 323, 383
———. 2002b, Nature, 420, 390
Wang, H., Zirin, H., & Ai, G. 1991, Sol. Phys., 131, 53
Weiss, N. O., Thomas, J. H., Brummell, N. H., & Tobias, S. M. 2004, ApJ, 600, 1073
Westendorp Plaza, C., del Toro Iniesta, J. C., Ruiz Cobo, B., & Pillet, V. M. 2001a, ApJ, 547, 1148
Westendorp Plaza, C., del Toro Iniesta, J. C., Ruiz Cobo, B., Pillet, V. M., Lites, B. W., & Skumanich, A. 2001b, ApJ, 547, 1130
———. 1986, Sol. Phys., 106, 1
Yurchyshyn, V. B., & Wang, H. 2001, Sol. Phys., 202, 309
Yurchyshyn, V. B., Wang, H., & Goode, P. R. 2001, ApJ, 550, 470
Zhang, H., Ai, G., Wang, H., Zirin, H., & Patterson, A. 1992, Sol. Phys., 140, 307
Zhang, J., Solanki, S. K., & Wang, J. 2003, A&A, 399, 755